

A 2D hybrid stress element for improved prediction of the out-of-plane fields using Fourier expansion

M. L. Feng[†] and M. Dhanasekar[‡]

*Faculty of Engineering and Physical Systems, Central Queensland University,
Rockhampton MC QLD 4702, Australia*

Q. Z. Xiao^{‡†}

*Department of Modern Mechanics, University of Science and Technology of China,
Hefei, 230026, People's Republic of China*

(Received June, 2001, Accepted March, 2002)

Abstract. Recently we formulated a 2D hybrid stress element from the 3D Hellinger-Reissner principle for the analysis of thick bodies that are symmetric to the thickness direction. Polynomials have typically been used for all the displacement and stress fields. Although the element predicted the dominant stress and all displacement fields accurately, its prediction of the out-of-plane shear stresses was affected by the very high order terms used in the polynomials. This paper describes an improved formulation of the 2D element using Fourier series expansion for the out-of-plane displacement and stress fields. Numerical results illustrate that its predictions have markedly improved.

Key words: hybrid stress element; out-of-plane fields; plane deformation; Fourier-series expansion; 3-D elastic theory.

1. Introduction

In engineering, classical plane stress and plane strain hypotheses are commonly used for the analysis of structures depending on their geometric characteristics and the type of loading. Thickness of the structure plays a major role in the modelling of bodies subjected to inplane loading. When the thickness is too small, plane stress condition applies, while it is too large, plane strain condition applies. When the thickness is comparable to other dimensions (i.e., neither too small, nor too large), three-dimensional analysis becomes inevitable.

Recently Ye (1997) presented a 2D isoparametric element for the prediction of 3D stress and displacement fields from 2D analysis. We have improved Ye's formulation for the analysis of homogeneous deformable bodies (either solid or hollow) with moderate thickness that are symmetric to their thickness direction (Xiao and Dhanasekar 2000, Dhanasekar and Xiao 2001). Our improved

[†] Post Doctoral Fellow

[‡] Senior Lecturer

^{‡†} Visiting Scholar-CQU, Australia

formulation yielded a four node 2D hybrid stress element with six degrees of freedom per node, which we termed as a quasi 3D element with 24 stress parameters (Q3D24 β). We formulated the element Q3D24 β using polynomial series expansion for the distribution of the stress and displacement fields. Higher order terms (such as z^4 and z^5) were used in the polynomials defining the out-of-plane shear stresses with a view to satisfying the anti-symmetric distribution of the fields about the mid-plane and to eliminate the spurious modes of rank insufficiency of the eigenvalue of the stiffness matrices. Furthermore, traction free conditions on the two external lateral surfaces have been specifically enforced by appropriate selection of the terms of the polynomials. Traction free conditions are particularly important for the plane stress bodies to satisfy the compatibility equations.

The quasi 3D element Q3D24 β predicted all the displacement and the dominant stress fields satisfactorily. However, the magnitude of the out-of-plane shear stresses τ_{yz} , τ_{zx} is generally predicted less accurately in comparison with the results of 3D analysis using ABAQUS.

This paper describes an improved re-formulation of the Q3D24 β element by using Fourier-series expansion for the out-of-plane (both the displacement and stress) fields. Traction free conditions on the external lateral surfaces that are perpendicular to the thickness direction have been imposed in the assumption of the Fourier series stress function. A new four-node plane hybrid stress element with 24 stress parameters has thus been formulated from the 3D Hellinger-Reissner principle and is termed as Q3D24 β F in this paper.

A cube shaped elastic cantilever solid example has been used to validate the results of the Q3D24 β F element in comparison to the Q3D24 β element and the 3D results from ABAQUS.

2. Displacement and stress fields assumption based on Fourier series expansion

Consider a solid with a plane of symmetry xy as shown in Fig. 1. Without loss of generality, the x - and y -axes are located at the mid-section, and the z -axis along the thickness direction. According to the modified theory of the plane stress state (Ye 1997, Timoshenko and Goodier 1970), the in-plane displacement components u , v and the stress components σ_x , σ_y , τ_{xy} , σ_z are symmetric to the middle section while the lateral displacement w and the out-of-plane shear stresses τ_{yz} , τ_{zx} are anti-symmetric to the middle (xy) plane when the solid is structurally symmetric to the middle xy plane and subjected to only inplane loading.

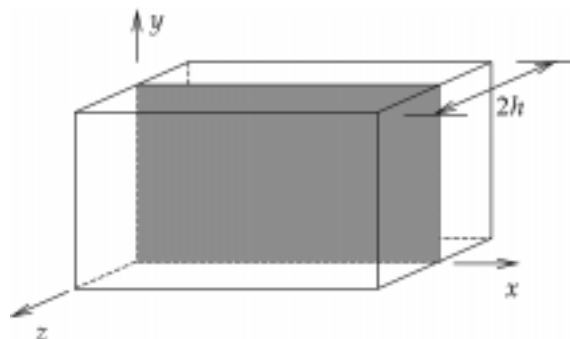


Fig. 1 A symmetric solid and coordinate system

$$\Pi_{HR}^{(e)}(u, \sigma) = \int_{-h}^h \left\{ \int_{A^{(e)}} \left[-\frac{1}{2} \sigma^T S \sigma + \sigma^T (Du) \right] dA - \int_{A^{(e)}} \bar{f}^T u dA - \int_{S_\sigma^{(e)}} \bar{T}^T u ds \right\} dz \quad (4)$$

where $u = [u \ v \ w]^T$ and $\sigma = [\sigma_x \ \sigma_y \ \tau_{xy} \ \tau_{yz} \ \tau_{zx} \ \sigma_z]^T$. S is the compliance matrix, D is the differential operator matrix. $A^{(e)}$ is the area of element 'e', $S_\sigma^{(e)}$ the part of the element boundary on which traction is prescribed. \bar{T} and \bar{f} are the surface and volumetric force vector respectively.

Consider an element with n nodes and six degrees of freedom at each node. The displacement of the element u is related to nodal values q via the shape functions N

$$u = Nq \quad (5)$$

in which,

$$q^T = [q^{(1)T} \ q^{(2)T} \ \dots \ q^{(n)T}]$$

$$N = [N^{(1)} \ N^{(2)} \ \dots \ N^{(n)}] \quad (6)$$

The nodal values and shape functions for an arbitrary node i are

$$q^{(i)} = [u_0^{(i)} \ u_1^{(i)} \ v_0^{(i)} \ v_1^{(i)} \ w_0^{(i)} \ w_1^{(i)}] \quad (7)$$

$$N^{(i)} = \begin{bmatrix} N_i z^2 N_i & 0 & 0 & 0 & 0 & 0 \\ 0 & 0 & N_i z^2 N_i & 0 & 0 & 0 \\ 0 & 0 & 0 & 0 & z N_i \sin(\pi \bar{z}) N_i & 0 \end{bmatrix} \quad (8)$$

where u_0, v_0, w_0 and u_1, v_1, w_1 are terms in the displacement polynomials (u, v, w) given in Eq. (1).

The strain array relevant to Eq. (5) is

$$\varepsilon = Du = Bq \quad (9)$$

where $B = [B^{(1)} \ B^{(2)} \ \dots \ B^{(n)}]$. For an arbitrary node i ,

$$B^{(i)} = B_0^{(i)} + z B_1^{(i)} + z^2 B_2^{(i)} + \sin(\pi \bar{z}) B_3^{(i)} + \cos(\pi \bar{z}) B_4^{(i)} \quad (10)$$

and

$$B_0^{(i)} = \begin{bmatrix} N_{i,x} & 0 & 0 & 0 & 0 & 0 \\ 0 & 0 & N_{i,y} & 0 & 0 & 0 \\ N_{i,y} & 0 & N_{i,x} & 0 & 0 & 0 \\ 0 & 0 & 0 & 0 & 0 & 0 \\ 0 & 0 & 0 & 0 & 0 & 0 \\ 0 & 0 & 0 & 0 & N_i & 0 \end{bmatrix} \quad B_1^{(i)} = \begin{bmatrix} 0 & 0 & 0 & 0 & 0 & 0 \\ 0 & 0 & 0 & 0 & 0 & 0 \\ 0 & 0 & 0 & 0 & 0 & 0 \\ 0 & 0 & 0 & 2N_i & N_{i,y} & 0 \\ 0 & 2N_i & 0 & 0 & N_{i,x} & 0 \\ 0 & 0 & 0 & 0 & 0 & 0 \end{bmatrix}$$

$$B_2^{(i)} = \begin{bmatrix} 0 & N_{i,x} & 0 & 0 & 0 & 0 \\ 0 & 0 & 0 & N_{i,y} & 0 & 0 \\ 0 & N_{i,y} & 0 & N_{i,x} & 0 & 0 \\ 0 & 0 & 0 & 0 & 0 & 0 \\ 0 & 0 & 0 & 0 & 0 & 0 \\ 0 & 0 & 0 & 0 & 0 & 0 \end{bmatrix} \quad B_3^{(i)} = \begin{bmatrix} 0 & 0 & 0 & 0 & 0 & 0 \\ 0 & 0 & 0 & 0 & 0 & 0 \\ 0 & 0 & 0 & 0 & 0 & 0 \\ 0 & 0 & 0 & 0 & 0 & N_{i,y} \\ 0 & 0 & 0 & 0 & 0 & N_{i,x} \\ 0 & 0 & 0 & 0 & 0 & 0 \end{bmatrix}$$

$$B_4^{(i)} = \begin{bmatrix} 0 & 0 & 0 & 0 & 0 & 0 \\ 0 & 0 & 0 & 0 & 0 & 0 \\ 0 & 0 & 0 & 0 & 0 & 0 \\ 0 & 0 & 0 & 0 & 0 & 0 \\ 0 & 0 & 0 & 0 & 0 & 0 \\ 0 & 0 & 0 & 0 & 0 & \frac{\pi}{h} N_i \end{bmatrix}$$

The stress is related to the stress parameters β via the stress interpolation function φ

$$\sigma = \varphi\beta \tag{11}$$

where

$$\varphi = \begin{bmatrix} \varphi_{x0} & \bar{z}^2 \varphi_{x1} & 0 & 0 \\ \varphi_{y0} & \bar{z}^2 \varphi_{y1} & 0 & 0 \\ \varphi_{xy0} & \bar{z}^2 \varphi_{xy1} & 0 & 0 \\ 0 & 0 & \bar{z} [1 + \cos(\pi\bar{z})] \varphi_{yz0} & \bar{z}^3 [1 + \cos(\pi\bar{z})] \varphi_{yz1} \\ 0 & 0 & \bar{z} [1 + \cos(\pi\bar{z})] \varphi_{zx0} & \bar{z}^3 [1 + \cos(\pi\bar{z})] \varphi_{zx1} \\ 0 & 0 & \frac{[1 + \cos(\pi\bar{z})]}{2} \varphi_{z0} & \bar{z}^2 \frac{[1 + \cos(\pi\bar{z})]}{2} \varphi_{z1} \end{bmatrix} \tag{12}$$

$$= \left[\varphi_0 \bar{z}^2 \varphi_1 \bar{z} [1 + \cos(\pi\bar{z})] f(z) \varphi_2 + \frac{[1 + \cos(\pi\bar{z})]}{2} \varphi_3 \bar{z}^3 [1 + \cos(\pi\bar{z})] f(z) \varphi_4 + \bar{z}^2 [1 + \cos(\pi\bar{z})] f(z) \varphi_5 \right]$$

where,

$$\varphi_0 = \begin{bmatrix} \varphi_{x0} \\ \varphi_{y0} \\ \varphi_{xy0} \\ 0 \\ 0 \\ 0 \end{bmatrix} \quad \varphi_1 = \begin{bmatrix} \varphi_{x1} \\ \varphi_{y1} \\ \varphi_{xy1} \\ 0 \\ 0 \\ 0 \end{bmatrix} \quad \varphi_2 = \begin{bmatrix} 0 \\ 0 \\ 0 \\ \varphi_{yz0} \\ \varphi_{zx0} \\ 0 \end{bmatrix} \quad \varphi_3 = \begin{bmatrix} 0 \\ 0 \\ 0 \\ 0 \\ 0 \\ \varphi_{z0} \end{bmatrix} \quad \varphi_4 = \begin{bmatrix} 0 \\ 0 \\ 0 \\ \varphi_{yz1} \\ \varphi_{zx1} \\ 0 \end{bmatrix} \quad \varphi_5 = \begin{bmatrix} 0 \\ 0 \\ 0 \\ 0 \\ 0 \\ \varphi_{z1} \end{bmatrix} \tag{13}$$

Substituting Eqs. (5), (9) and (11) into Eq. (4), and making use of the stationary condition, we obtain

$$\beta = H^{-1}Gq \quad (14)$$

and the discrete equations of equilibrium of element ‘e’

$$K^{(e)}q = \bar{f}^{(e)} \quad (15)$$

where the stiffness matrix of element ‘e’ is

$$K^{(e)} = G^T H^{-1} G \quad (16)$$

The corresponding load vector is,

$$\bar{f}^{(e)} = \int_{-h}^h \left\{ \int_{A^{(e)}} N^T \bar{f}^{(e)} dA + \int_{S_{\sigma}^{(e)}} N^T \bar{T} ds \right\} dz \quad (17)$$

Here the characteristic matrices of the element are,

$$H = \int_{-h}^h \int_{A^{(e)}} \varphi^T S \varphi dA dz, \quad G = \int_{-h}^h \int_{A^{(e)}} \varphi^T B dA dz \quad (18)$$

In the area $A^{(e)}$ of the xy plane, we carry out the integration in Eq. (18) using the traditional numerical Gauss integration rule. However, as the out-of-plane functions were relatively easily integrable, we integrate the matrices in Eq. (18) analytically in the z -direction (‘thickness’ direction). The integrals along the z -direction are given as follows:

$$\int_{-h}^h \varphi^T S \varphi dz = 2h \begin{bmatrix} c_0 \varphi_0^T S \varphi_0 & c_1 \varphi_0^T S \varphi_1 & c_7 \varphi_0^T S \varphi_3 & c_6 \varphi_0^T S \varphi_5 \\ & c_2 \varphi_1^T S \varphi_1 & c_6 \varphi_1^T S \varphi_3 & \frac{1}{2} c_5 \varphi_1^T S \varphi_5 \\ & & c_{10} \varphi_2^T S \varphi_2 + c_{13} \varphi_3^T S \varphi_3 & \frac{1}{4} c_{10} \varphi_3^T S \varphi_5 + c_{11} \varphi_2^T S \varphi_4 \\ \text{Sym.} & & & c_{12} \varphi_4^T S \varphi_4 + \frac{1}{4} c_{11} \varphi_5^T S \varphi_5 \end{bmatrix}$$

$$\int_{-h}^h \varphi^T B^{(i)} dz = 2h \begin{bmatrix} c_0 \varphi_0^T B_0^{(i)} + c_1 \varphi_0^T B_2^{(i)} h^2 \\ c_1 \varphi_1^T B_0^{(i)} + c_2 \varphi_1^T B_2^{(i)} h^2 - c_3 \varphi_1^T B_4^{(i)} \\ \varphi_2^T (2c_6 B_1^{(i)} h + c_4 B_3^{(i)}) + \varphi_3^T \left(c_6 B_2^{(i)} h^2 + c_7 B_0^{(i)} + \frac{1}{2} c_7 B_4^{(i)} \right) \\ \varphi_4^T (c_8 B_3^{(i)} + c_5 B_1^{(i)} h) + \varphi_5^T \left(\frac{1}{2} c_5 B_2^{(i)} h^2 + c_6 B_0^{(i)} + c_9 B_4^{(i)} \right) \end{bmatrix} \quad (19)$$

in which

$$c_0 = 1; \quad c_1 = \frac{1}{3}; \quad c_2 = \frac{1}{5}; \quad c_3 = -\frac{2}{\pi};$$

$$c_4 = \frac{3}{4\pi}; \quad c_5 = \frac{\pi^4 - 20\pi^2 + 120}{5\pi^4}; \quad c_6 = \frac{\pi^2 - 6}{6\pi^2};$$

$$c_7 = \frac{1}{2}; \quad c_8 = \frac{6\pi^2 - 45}{8\pi^3}; \quad c_9 = \frac{2\pi^2 - 21}{24\pi^2}; \quad c_{10} = \frac{2\pi^2 - 15}{4\pi^2};$$

$$C_{11} = \frac{6\pi^4 - 150\pi^2 + 945}{20\pi^4}; \quad C_{12} = \frac{3(-26775 - 4410\pi^2 - 210\pi^4 + 4\pi^6)}{56\pi^6}; \quad C_{13} = \frac{3}{8}$$

As defined by Wu and Bufler (1991), Eq. (15) could not be solved uniquely unless the displacement and stress parameters are selected appropriately that satisfy the condition given in Eq. (20).

$$n_\beta \geq n_q - n_r \tag{20}$$

where n_β and n_q represent the number of element stress and nodal displacement parameters, respectively and n_r is the number of independent rigid body motions which is equal to 3 in the current case. This means although Q3D24βF is a quasi 3D element, only three rigid body motions in the xy plane are required to be suppressed similar to any other 2D element.

In the formulation of the hybrid stress element, the performance, or the capability of the element in predicting stresses were improved through the introduction of incompatible displacements (Wu and Bufler 1991, Wu and Cheung 1995). We added an incompatible displacement field each (as shown in Eq. (21)) to the compatible displacement field in Eq. (1).

$$u_\lambda(x, y, z) = u_{0\lambda}(x, y) + z^2 u_{1\lambda}(x, y)$$

$$v_\lambda(x, y, z) = v_{0\lambda}(x, y) + z^2 v_{1\lambda}(x, y)$$

$$w_\lambda(x, y, z) = z w_{0\lambda}(x, y) + \sin(\pi z) w_{1\lambda}(x, y) \tag{21}$$

Substituting the field into Eq. (4). The stationary condition of the functional provided equilibrium, compatibility, equilibrium of traction between elements and the prescribed traction constraints when the integral shown in Eq. (22) vanished.

$$\int_{-h}^h \oint_{\partial A^{(e)}} \sigma^T n^T \delta u_\lambda ds dz = 0 \tag{22}$$

in which $\partial A^{(e)}$ is the boundary of the element, and n is the matrix of the direction cosines of the unit outward normal to the element boundary.

In this derivation we have used the condition of traction free state on the external lateral surfaces. By explicitly integrating (22) and by letting the terms of $u_0, v_0, w_0, \sigma_{x0}, \sigma_{y0}, \tau_{xy0}, \tau_{yz0}$ and τ_{zx0} same as that for $u_1, v_1, w_1, \sigma_{x1}, \sigma_{y1}, \tau_{xy1}$, and τ_{yz1} , we obtain the patch test conditions (PTC) as shown in Eq. (23) for evaluating the incompatible displacement fields that pass the PTC,

$$\begin{aligned} \oint_{\partial A^{(e)}} (\sigma_{x0c}n_1 + \tau_{xy0c}n_2)u_{0\lambda}ds &= 0 \\ \oint_{\partial A^{(e)}} (\tau_{xy0c}n_1 + \sigma_{y0c}n_2)v_{0\lambda}ds &= 0 \\ \oint_{\partial A^{(e)}} (\tau_{zx0c}n_1 + \tau_{yz0c}n_2)w_{0\lambda}ds &= 0 \end{aligned} \tag{23}$$

and the stress optimisation conditions (OPC) as shown in Eq. (24) for optimising the trial stresses, as discussed in Wu and Bufler (1991), Wu and Cheung (1995).

$$\begin{aligned} \oint_{\partial A^{(e)}} (\sigma_{x0h}n_1 + \tau_{xy0h}n_2)u_{0\lambda}ds &= 0 \\ \oint_{\partial A^{(e)}} (\tau_{xy0h}n_1 + \sigma_{y0h}n_2)v_{0\lambda}ds &= 0 \\ \oint_{\partial A^{(e)}} (\tau_{zx0h}n_1 + \tau_{yz0h}n_2)w_{0\lambda}ds &= 0 \end{aligned} \tag{24}$$

It should be noted that the PTC above supercedes the traditional Babuska-Brezzi (BB) condition as proved by Wu and Buffer (1991), Wu and Pian (1997). Therefore, as the Q3D24βF element satisfies PTC, the element is stable and is guaranteed to provide converging results with mesh refinement similar to the Q3D24β element (Dhanasekar and Xiao 2001).

4. A 4-noded hybrid stress element

With reference to the usual 4-noded isoparametric element shown in Fig. 2, the shape functions employed in Eq. (8) are widely used bilinear interpolation functions

$$N_i = \frac{1}{4}(1 + \xi_i\xi)(1 + \eta_i\eta) \tag{25}$$

where (ξ, η) represent the isoparametric coordinates, (ξ_i, η_i) represent the isoparametric coordinates of point i with the global coordinates (x_i, y_i) , $i = 1, 2, 3, 4$.

It is easy to prove that the patch test condition (PTC) and stress optimisation condition (OPC) formulae in the current case are the same as those derived in Dhanasekar and Xiao (2001). Thus

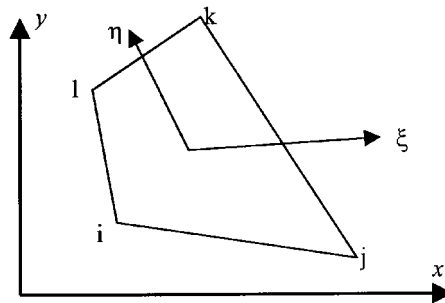


Fig. 2 A four node isoparametric 2D element

trial stresses in Dhanasekar and Xiao (2001) are adopted here directly. We thus have the stress interpolation function for plane stress components

$$\begin{bmatrix} \varphi_{x0} \\ \varphi_{y0} \\ \varphi_{xy0} \end{bmatrix} = \begin{bmatrix} \varphi_{x1} \\ \varphi_{y1} \\ \varphi_{xy1} \end{bmatrix} = \begin{bmatrix} 1 & 0 & 0 & a_1^2 \eta & a_3^2 \xi \\ 0 & 1 & 0 & b_1^2 \eta & b_3^2 \xi \\ 0 & 0 & 1 & a_1 b_1 \eta & a_3 b_3 \xi \end{bmatrix} \quad (26a)$$

which are that of the plane hybrid stress element PS (Pian and Sumihara 1984), and

$$\begin{bmatrix} \varphi_{yz0} \\ \varphi_{zx0} \\ \varphi_{z0} \end{bmatrix} = \begin{bmatrix} \varphi_{yz1} \\ \varphi_{zx1} \\ \varphi_{z1} \end{bmatrix} = \begin{bmatrix} 1 & 0 & b_1 \eta & b_3 \xi & 0 & 0 & 0 \\ 0 & 1 & a_1 \eta & a_3 \xi & 0 & 0 & 0 \\ 0 & 0 & 0 & 0 & 1 & \xi & \eta \end{bmatrix} \quad (26b)$$

where coefficients a_i and b_i ($i = 1, 2, 3$) are dependent on the element nodal coordinates as follows:

$$\begin{bmatrix} a_1 & b_1 \\ a_2 & b_2 \\ a_3 & b_3 \end{bmatrix} = \frac{1}{4} \begin{bmatrix} -1 & 1 & 1 & -1 \\ 1 & -1 & 1 & -1 \\ -1 & -1 & 1 & 1 \end{bmatrix} \begin{bmatrix} x_1 & y_1 \\ x_2 & y_2 \\ x_3 & y_3 \\ x_4 & y_4 \end{bmatrix} \quad (27)$$

In the element formulation discussed in Section 3, we define N_i by Eq. (26) and use the assumed displacements in Eq. (5) and the trial stresses in Eq. (11). Eq. (26) is used as the stress interpolation functions of plane components and out-of-plane components. The resulting quasi 3D element has 24 stress parameters (β), and is therefore designated as Q3D24 β F.

For the current element, $n_\beta = 24$, $n_q = 24$, and hence the element meets the stability condition of Eq. (20). A 2×2 Gauss quadrature is employed for the element formulation. Theoretical analysis and results of eigenvalue checks show that the element is rank-sufficient. Convergence check using h -refinement has shown rapid convergence of the dominant displacement and stress fields.

5. Numerical results

In this section, to validate the 2D-hybrid stress element Q3D24 β F, we compare the results of the current element Q3D24 β F with our previous element Q3D24 β and an eight node 3D hybrid stress element in ABAQUS.

A cube shaped elastic cantilever solid of dimension $2 \times 2 \times 2$ shown in Fig. 3 was considered as the example problem (the same problem was previously used to validate our original Q3D24 β element). The values of material properties and loading used in this example conform to those used for the flexural cantilever beam problem normally employed for checking of the h -refinement (Wu and Pian 1997). Accordingly the Young's modulus and the Poisson's ratio of the solid were kept as 1500 and 0.25 respectively.

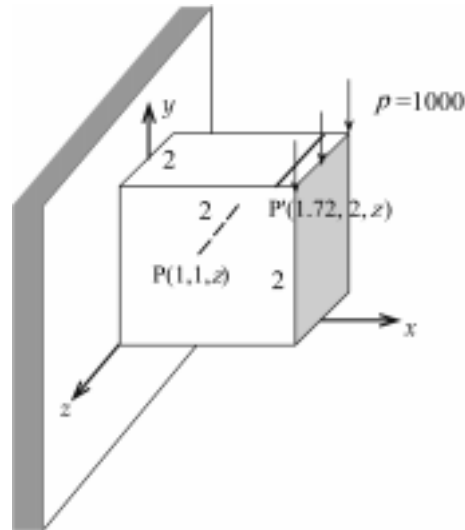


Fig. 3 A cubic cantilever beam

The origin of the coordinate system was chosen at the lower left edge of the middle plane of the cube. The xy plane defined the middle section of the cube and z -axis defined its thickness direction (from -1 to $+1$). The left yz plane was fixed and the vertical load was applied at the top edge of the right yz plane in the $-y$ direction. The vertical load was 1000 per unit length with its unit consistent with that of the Young's modulus.

Due to symmetry about the xy plane, only half of the solid was used in the 3D ABAQUS analysis. A $8 \times 8 \times 16$ mesh with 1024 brick elements and 1377 nodes was used in the 3D analysis. The displacement and stress components were monitored at the centre of the solid ($x = 1.0$, $y = 1.0$, $z = 0$ to 1.0) as shown in Fig. 3.

The same problem was then modelled using the 2D hybrid stress elements Q3D24 β F. Only the middle section was required to be meshed in this case and a 8×8 mesh was used. The displacement and stress were monitored at a point P ($x = 1.0$, $y = 1.0$) that is the projected view of the trace of the above line on the xy plane. The variation of displacement and stress components through the thickness was then determined from Eqs. (1) and (3). Comparison of the results of the half solid obtained by a 3D analysis of the ABAQUS program and by the Q3D24 β and Q3D24 β F methods is presented in Table 1. The maximum and minimum values predicted by the three types of elements for all the stress and displacement fields are presented in the table. Also shown in the table (in columns E , F , L and M) are the % errors between the predicted values using Q3D24 β and Q3D24 β F elements in comparison to that obtained by the ABAQUS 3D element. The following observations may be made from the values in Table 1:

- The inplane stresses are significantly larger than the out-of-plane stresses along the path $(1.0, 1.0, z)$.
- The dominant stresses (whose values in the order of 100s) have been predicted with less than 5% error by both the Q3D24 β and Q3D24 β F elements.
- With the reduction in the values of the stresses, the % error has increased.
- There is a marked improvement in the % error in the out-of-plane shear stresses (τ_{yz} , τ_{zx}) due to

Table 1 Comparison of the prediction of the current element with the predictions of our previous element and a 3D ABAQUS element

| Field @ (1, 1, z) | Maximum Value | | | | |
|-----------------------------------|---------------|---------------|------------|-----------------------|-----------------------|
| | 3D_ABAQUS | 2D_Polynomial | 2D_Fourier | %Error: (C) to (B) | %Error: (D) to (B) |
| (A) | (B) | (C) | (D) | (E) | (F) |
| σ_{xx} | -222.00 | -221.48 | -223.76 | 0.24 | 0.79 |
| σ_{yy} | 117.00 | 118.63 | 114.13 | 1.39 | 2.45 |
| τ_{xy} | -792.00 | -756.79 | -761.16 | 4.45 | 3.89 |
| σ_{zz} | 2.00 | 1.67 | 1.12 | 16.45 | 44.18 |
| τ_{yz} | 0.00 | 0.00 | 0.00 | 0.00 | 0.00 |
| τ_{zx} | 0.61 | 0.28 | 0.47 | 53.97 | 22.38 |
| u | -0.0740 | -0.0804 | -0.0808 | 8.65 | 9.14 |
| v | -1.6700 | -1.6596 | -1.6636 | 0.62 | 0.38 |
| w | 0.0330 | 0.0325 | 0.0323 | 1.57 | 2.21 |
| σ_{zz} @ (1.72, 2.0, z) | 1370.00 | 1417.00 | 1343.70 | 3.43 | 1.92 |
| Field @ (1, 1, z) | Minimum Value | | | | |
| | 3D_ABAQUS | 2D_Polynomial | 2D_Fourier | %Error: (H) to (G) | %Error: (K) to (G) |
| (A) | (G) | (H) | (K) | (L) | (M) |
| σ_{xx} | -351.00 | -347.61 | -342.69 | 0.97 | 2.37 |
| σ_{yy} | 38.00 | 41.48 | 43.96 | 9.15 | 15.67 |
| τ_{xy} | -887.50 | -910.82 | -902.18 | 2.63 | 1.65 |
| σ_{zz} | -3.90 | -3.62 | -3.38 | 7.30 | 13.46 |
| τ_{yz} | -28.50 | -20.71 | -23.11 | 27.33 | 18.92 |
| τ_{zx} | -0.37 | -1.16 | -0.31 | 213.66 | 15.45 |
| u | -0.1340 | -0.1410 | -0.1407 | 5.22 | 5.03 |
| v | -1.7580 | -1.7600 | -1.7600 | 0.11 | 0.11 |
| w | -0.0330 | -0.0325 | -0.0323 | 1.57 | 2.21 |
| σ_{zz} @ (1.72, 2.0, z) | 0.00 | 0.00 | 0.00 | 0.00 | 0.00 |

the Fourier expansion based element Q3D24 β F compared to the polynomial expansion based element Q3D24 β .

- The displacements (u , v , w) predicted by all the three elements are in good agreement with each other with the % error remaining less than 10%. There is very little difference between the predictions of the Q3D24 β and Q3D24 β F elements.

As the out-of-plane normal stress (σ_z) at the centre of the cube (1.0, 1.0, z) is very small, it is difficult to conclude on the benefits of using the Q3D24 β F element. Indeed from the data presented in Table 1 for σ_z it might appear that the prediction of the Q3D24 β F element is worse than the Q3D24 β element. To ensure that this was due to the extremely smaller values at (1.0, 1.0, z), a

search in ABAQUS was made to select a path with higher values of σ_z . The path (1.72, 2.0, z) provided the maximum out-of-plane normal stress σ_z . This path is also shown in Fig. 3.

The values of σ_z predicted by Q3D24 β and Q3D24 β F along the path (1.72, 2.0, z) are in good agreement with the 3D analysis of ABAQUS. The maximum % error is only 3.43% using the element Q3D24 β . The Q3D24 β F element has exhibited even a smaller error of 1.92%. The purpose of selecting the additional path (1.72, 2.0, z) is only to ensure that the use of Fourier series does not adversely affect the dominant stress fields (σ_x , σ_y , τ_{xy} , σ_z). The merit of the use of Fourier series expansion for the out-of-plane fields should only be inferred from the two out-of-plane shear stresses that were predicted poorly by the element Q3D24 β . To further illustrate this point, the distribution of τ_{yz} , τ_{zx} predicted by the three element along the path (1.0, 1.0, z) is shown in Figs. 4 and 5 respectively. The benefit of using Fourier series expansion becomes evident from these two graphs.

6. Conclusions

A semi analytical plane, quasi 3D hybrid stress element based on Fourier series expansion (Q3D24 β F) was developed from the 3D Hellinger-Reissner principle for solids of uniform thickness that possess structural symmetry to its middle plane. The element was formulated similar to the Q3D24 β element reported previously (Xiao and Dhanasekar 2000). In the formulation of Q3D24 β F, we used polynomials for the distribution of the inplane displacement (u , v) and stress (σ_x , σ_y , τ_{xy}) fields and Fourier series expansion for the out-of-plane displacement (w) and stress (σ_z , τ_{yz} , τ_{zx})

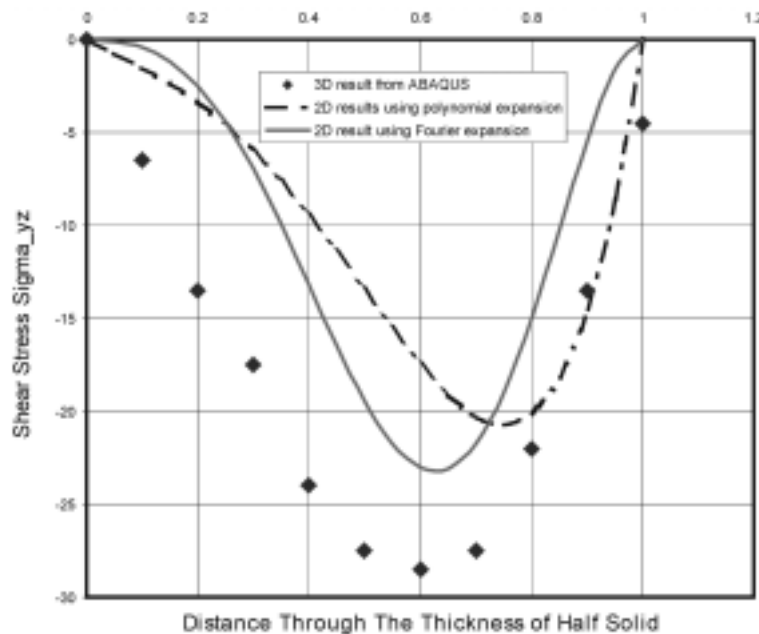


Fig. 4 Comparison of the distribution of τ_{yz} by the current element with the predictions of our previous element and a 3D ABAQUS element

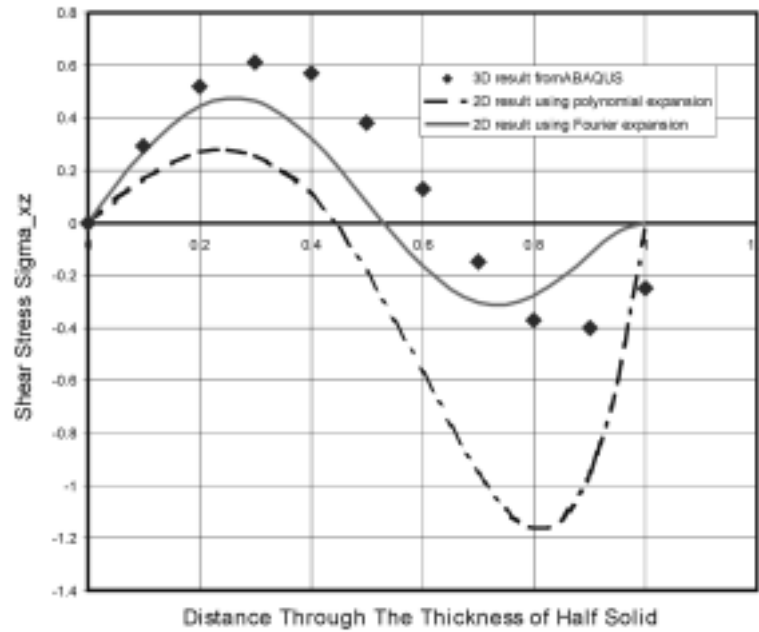


Fig. 5 Comparison of the distribution of τ_{zx} by the current element with the predictions of our previous element and a 3D ABAQUS element

fields. Traction free conditions on the external surfaces perpendicular to the axis passing through the thickness direction were enforced in the selection of the stresses in terms of the polynomial and Fourier series expansion.

The element Q3D24 β F predicted accurate results of all displacements (u , v , w) and dominant stresses (σ_x , σ_y , τ_{xy} , σ_z) similar to Q3D24 β . It improved the prediction of the out-of-plane shear stresses (τ_{yz} , τ_{zx}) markedly. It is therefore concluded that there is advantage in using Fourier series expansion for the out-of-plane displacement and stress fields rather than the traditional polynomial series. The current Q3D24 β F element is therefore, considered superior to our earlier Q3D24 β element.

Acknowledgements

The authors acknowledge the generous support of CQU in offering funding under the Research Advancement Award Scheme (RAAS) to the Second author. The grant has made it possible for the first author to take part in the research.

References

- Dhanasekar M. and Xiao Q.Z. (2001), "Plane hybrid stress element method for 3D hollow bodies of uniform thickness", *Computers and Structures*, **79**, 483-497.
 Pian T.H.H. and Wu C.C. (1988), "A rational approach for choosing stress terms for hybrid finite element

- formulations”, *Int. J. Numer. Meth. Engng.*, **26**, 2331-2343.
- Pian T.H.H. and Sumihara K. (1984), “Rational approach for assumed stress finite elements”, *Int. J. Numer. Meth. Engng.*, **20**, 1685-1695.
- Timoshenko S.P. and Goodier J.N. (1970), *Theory of Elasticity*, 3rd. McGraw-Hill.
- Wu C.C. and Bufler H. (1991), “Multivariable finite elements: consistency and optimization”, *Science in China(A)* **34**, 284-299.
- Wu C.C. and Cheung Y.K. (1995), “On optimisation approaches of hybrid stress elements”, *Finite Elements Anal. Des.*, **21**, 111-128.
- Wu C.C. and Pian T.H.H. (1977), *Numerical Analysis Method of Incompatible and Hybrid Elements (in Chinese)*, China Science Press.
- Xiao Q.Z. and Dhanasekar M. “Plane hybrid stress element for 3D problems”, *Proc. of the 5th Int. Conf. on Computational Structures Technology*, Leuven, Belgium, Sep 2000; *Finite Elements Techniques and Development*-edited by Topping B.H.V.; Civil-Comp Press; 147-158.
- Ye Z.M. (1997), “A new finite element formulation for planar elastic deformation”, *Int. J. Numer. Meth. Eng.*, **40**, 2579-2591.